

# On the auxetic properties of generic rotating rigid triangles

BY JOSEPH N. GRIMA<sup>1,\*</sup>, ELAINE CHETCUTI<sup>1</sup>, ELAINE MANICARO<sup>1</sup>,  
DAPHNE ATTARD<sup>1</sup>, MATTHEW CAMILLERI<sup>1</sup>, RUBEN GATT<sup>1</sup>  
AND KENNETH E. EVANS<sup>2</sup>

<sup>1</sup>*Metamaterials Unit, Faculty of Science, University of Malta,  
Msida MSD 2080, Malta*

<sup>2</sup>*College of Engineering, Mathematics and Physical Sciences,  
University of Exeter, North Park Road, Exeter EX4 4QF, UK*

Materials having a negative Poisson's ratio (auxetic) get fatter rather than thinner when uniaxially stretched. This phenomenon has been often explained through models that describe how particular geometric features in the micro or nanostructure of the material deform when subjected to uniaxial loads. Here, a new model based on scalene rigid triangles rotate relative to each other will be presented and analysed. It is shown that this model can afford a very wide range of Poisson's ratio values, the sign and magnitude of which depends on the shape of the triangles and the angles between them. This new model has the advantage that it is very generic and may be potentially used to describe the properties in various types of materials, including auxetic foams and their relative surface density. Specific applications of this model, such as a blueprint for a system that can exhibit temperature-dependent Poisson's ratios, are also discussed.

**Keywords:** auxetic; negative Poisson's ratio; analytical model; foams; relative surface density

## 1. Introduction

Auxetic materials, unlike conventional materials, expand transversely when uniaxially stretched and contract in width when uniaxially compressed, i.e. exhibit a negative Poisson's ratio (Evans 1991). Apart from being unusual, these materials exhibit several enhanced properties, including higher resistance to indentation, the natural ability to adopt a dome-shape surface and high-energy absorption properties (Lakes 1987; Evans 1991; Lakes & Elms 1993; Alderson 1999; Scarpa & Tomlinson 2000; Scarpa & Smith 2004). These characteristics make auxetics suitable for the manufacture of various superior products ranging from pipes with enhanced shear modulus (Wadee *et al.* 2007) to more comfortable cushions that wrap better around human body parts while also offering higher protection as a result of their enhanced indentation resistance (Evans 1991). Other proposed that products made from auxetic components include specially designed 'expanding blast-proof curtains' made using auxetic fibres aimed at

\*Author for correspondence ([joseph.grima@um.edu.mt](mailto:joseph.grima@um.edu.mt)).

Electronic supplementary material is available at <http://dx.doi.org/10.1098/rspa.2011.0273> or via <http://rspa.royalsocietypublishing.org>.

protecting people in an explosion by capturing debris from smashed glass (EPSRC 2010), smart medical dressings that release medication in proportion to the extent of swelling (Alderson 1999) and several components of aircrafts, naval vessels and automobiles (Burke 1997).

Over the past few decades, several naturally existing auxetics have been discovered. These include biomaterials such as cow teat skin (Lees *et al.* 1991) and cat skin (Veronda & Westmann 1970), as well as inorganic materials such as silicates (Yeganeh-Haeri *et al.* 1992; Alderson *et al.* 2005; Grima *et al.* 2005), zeolites (Grima *et al.* 2000, 2007a) and metals (Baughman *et al.* 1998). In addition to these, several man-made auxetic materials have been designed and/or manufactured. These include auxetic foams (Lakes 1987; Chan & Evans 1997; Scarpa *et al.* 2004; Bezazi & Scarpa 2006; Grima *et al.* 2009), microporous or nanostructured polymers (Evans & Caddock 1989; Alderson *et al.* 1997; He *et al.* 1998) and fabrics (Hook *et al.* 2006; Liu *et al.* 2010). In all of these materials, the negative Poisson's ratio can be explained in terms of particular geometric features in the materials' micro or nanostructure (geometry) and the way these deform when a uniaxial stress is applied (the deformation mechanism), as is the case with most material where a certain mechanical property is correlated to the microstructure (Ashby *et al.* 1995; Gibson *et al.* 1995).

In fact, in an attempt to attain a better insight into the mechanisms that result in auxeticity, various geometry-based models have been proposed and developed not only to explain the observed negative Poisson's ratios in naturally occurring auxetic materials, but also to act as a blueprint for the design and manufacture of novel man-made auxetics. These include two-dimensional models based on the re-entrant hexagonal honeycomb structure (Gibson *et al.* 1982; Masters & Evans 1996) deforming through flexure and/or hinging, dilating structures (Masters & Evans 1996; Grima *et al.* 2008a), chiral structures (Wojciechowski & Branka 1989; Lakes 1991; Grima *et al.* 2008b), models based on rigid 'free' molecules (Wojciechowski 2003; Wojciechowski & Frenkel 2004) and 'rotating polygons' models based on rotating squares, triangles, rectangles, parallelograms or rhombi (Grima & Evans 2000a; Ishibashi & Iwata 2000; Grima *et al.* 2011). Three-dimensional models for auxetics include models based on rotating and/or dilating tetrahedra (Alderson & Evans 2002) and three-dimensional cells having re-entrant features (Evans *et al.* 1994; Choi & Lakes 1995). Here, it should be noted that although two-dimensional models have their obvious limitations when compared with three-dimensional models, their popularity lies in the fact that they are less complex to analyse, while at the same time often being adequate enough to predict the behaviour of particular two-dimensional projections of a more complex three-dimensional arrangement where the Poisson's ratios is being measured (the Poisson's ratio is a two-dimensional property).

In recent years, models based on rotating polygons have attracted considerable attention in view of their ability to explain the observed auxeticity in various materials ranging from zeolites to foams. For example, it has also been proposed that some zeolite-type frameworks may also exhibit negative Poisson's ratios as a result of nano-level deformations, which can be explained through rotating triangles or rotating square models where the triangles or squares represent the two-dimensional projection of the nano framework (Grima *et al.* 2000). Also, a recent study discussing rotating different-sized rectangles and squares suggests that a generic rotating rectangle model can be useful in describing the

properties of various materials such as liquid crystalline polymers and silicates (Grima *et al.* 2005, 2011). Furthermore, it has also been proposed that the concept of rotating triangles can be used to explain the experimentally measured negative Poisson's ratios in polymeric foams manufactured through the classic thermo-mechanical process (Lakes 1987) or the more recently proposed chemo-mechanical process (Grima *et al.* 2009). In such a description, the triangles represent the two-dimensional projection of the joints in the foam, which are proposed to behave like rigid units that rotate relative to each other (Grima *et al.* 2006), a hypothesis that is supported by three-dimensional X-ray microtomography (McDonald *et al.* 2010) and scanning electron microscope (SEM) images (Bianchi *et al.* 2010, 2011). However, although this concept marks an important step forward in elucidating the mechanisms that result in negative Poisson's ratio in auxetic foams, auxetics that are probably the closest to commercialization, the existent highly symmetric rotating triangle models (Grima & Evans 2006, 2010) cannot be used to realistically model the behaviour of foams because the microstructure of foams is too complex to describe it through highly symmetric models. In view of this, in an attempt to produce a more realistic and generic model that can better predict the behaviour of real auxetic materials, such as auxetic foams that may have rather irregular microstructures, here we propose and discuss a highly generic model built from scalene triangles. In particular, we derive the mechanical properties of systems made from tessellates of two non-equivalent scalene triangles connected together through their vertices via flexible hinges and show that amongst other things, this generic model can predict Poisson's ratios that are similar in magnitude to those measured in foams.

## 2. Generic analytical model

Referring to figure 1, the proposed model consists of two non-equivalent rigid scalene triangles with sides  $a_1, b_1, c_1$  and  $a_2, b_2, c_2$ , respectively, with corresponding interior angles  $\alpha_1, \beta_1, \gamma_1$  and  $\alpha_2, \beta_2, \gamma_2$ , where the interior angle  $\alpha_1$  lies opposite to the side of length  $a_1$  and similarly for the other interior angles. These triangles are connected through simple flexible hinges with angle  $\varphi$  at point A, angle  $\omega$  at point B and angle  $\theta$  at point C so as to form a tessellation (figure 1). For ease of reference, this system will be denoted by  $[a_1 \times b_1 \times c_1, a_2 \times b_2 \times c_2]$ .

Uniaxial tensile or compressive loading of such structures will result in a change in the angles  $\varphi, \omega, \theta$  between the triangles, which—as discussed below, for some particular combinations of the geometric variables and for particular directions of loading—result in a negative Poisson's ratios (figure 2).

Note that the angles  $\varphi, \omega$  and  $\theta$  are interdependent variables and can be rewritten in terms of each other and the internal angles of the triangles through,

$$\left. \begin{aligned} \varphi &= \theta - \alpha_1 + \gamma_2 = \omega + \beta_1 - \alpha_2 \\ \omega &= \theta + \gamma_1 - \beta_2 = \varphi - \beta_1 + \alpha_2 \\ \theta &= \omega - \gamma_1 + \beta_2 = \varphi + \alpha_1 - \gamma_2 \end{aligned} \right\}. \quad (2.1)$$

and

Also note that because it is being assumed that the triangles are perfectly rigid but may rotate relative to each other, then it is clear that for a given set of triangles the parameters  $a_1, b_1, c_1, a_2, b_2$  and  $c_2$  remain constant and, because

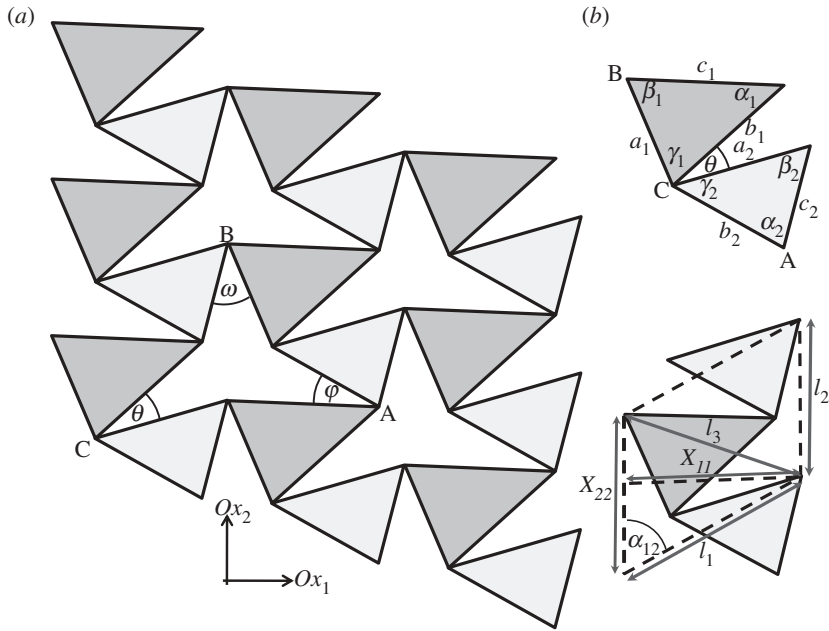


Figure 1. (a) The system made from connected different-sized scalene triangles of dimensions  $a_1 \times b_1 \times c_1$  and  $a_2 \times b_2 \times c_2$  (denoted by  $[a_1 \times b_1 \times c_1, a_2 \times b_2 \times c_2]$ ) discussed in this paper. (b) The parallelogramic unit cell where  $X_{22} = l_2$  is parallel to the  $Ox_2$  direction, whereas  $X_{11}$  is the projection of the unit cell in the  $Ox_1$  direction and  $\alpha_{12}$  is the unit cell angle.

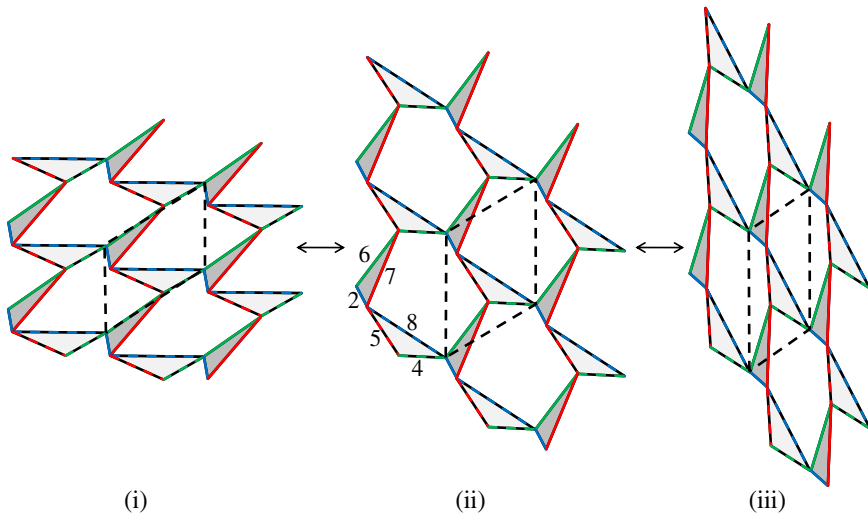


Figure 2. A typical deformation profile that may be obtained from the model proposed. Shown here is the deformation of the different-sized scalene triangles structure  $[2 \times 7 \times 6, 8 \times 5 \times 4]$ . Note that this structure is both auxetic and conventional, depending on the value of angle between the triangles. This figure is also provided as an animation (electronic supplementary material, see Anim-2). (Online version in colour.)

the parameters  $\varphi$ ,  $\omega$ ,  $\theta$  are interdependent variables, then the geometry of the system at any instant is only dependent on a single variable (e.g.  $\theta$ ).

Thus, as illustrated in figure 1, the shape and size of this system can be described in terms of  $\theta$  through a parallelogramic unit cell of side lengths  $l_1$ ,  $l_2$  and included angle  $\alpha_{12}$  given by

$$l_1 = \sqrt{c_1^2 + c_2^2 + 2c_1c_2 \cos(\theta - \alpha_1 - \beta_2)} \quad (2.2)$$

$$l_2 = \sqrt{b_1^2 + b_2^2 - 2b_1b_2 \cos(\theta + \gamma_2)} \quad (2.3)$$

and

$$\alpha_{12} = \cos^{-1} \left( \frac{l_1^2 + l_2^2 - l_3^2}{2l_1l_2} \right), \quad (2.4)$$

where  $l_3$  is the diagonal of the unit cell opposite to angle  $\alpha_{12}$ , which can be written as

$$l_3 = \sqrt{a_1^2 + a_2^2 - 2a_1a_2 \cos(\theta + \gamma_1)}. \quad (2.5)$$

For the purpose of this derivation, it will be assumed that the structure is aligned in such a way that the unit cell side of length  $l_2$  is always aligned parallel to the  $Ox_2$  direction while allowing the other unit cell side of length  $l_1$  to assume any direction. Here, it should be noted that there is no simple way how to experimentally determine the mechanical properties of real macrosystems with non-zero shear coupling coefficients such as the ones studied here because the standard mechanical property testing techniques are inappropriate for testing of such systems. In particular, under certain loading conditions, loading the structure in certain directions may cause the unit cell in figure 1 to rotate with respect to the global axis, something that is not catered for in this model. Nevertheless, the alignment assumed here is suitable for modelling of systems that undergo very small deformations, which are loaded in the appropriate manner so as to ensure that assumptions made here remain valid. Also, the imposition of an alignment constraint, such as the one imposed here, is essential as otherwise the system becomes indeterminate. In fact, it should be noted that this type of alignment is typical in the molecular modelling of crystals and is the standard alignment method used in a number of molecular modelling packages (e.g. CERIU<sup>2</sup>, Accelrys Inc.; Grima *et al.* 2000; Alderson *et al.* 2005).

With this proposed alignment, the projections of the unit cell in the  $Ox_1$  and  $Ox_2$  directions are, respectively, given by

$$X_{11} = l_1 \sin \alpha_{12} = \frac{\sqrt{4l_1^2l_2^2 - (l_1^2 + l_2^2 - l_3^2)^2}}{2l_2} \quad (2.6)$$

and

$$X_{22} = l_2 \quad (2.7)$$

Before proceeding any further, it should be noted that such tessellation is not necessarily space-filling. Also, not all structures for all angles are

physically realistic owing to overlapping of triangles. In fact, the hinging angle  $\theta$  for physically realistic structures where the triangles do not overlap must range between

$$\max(0^\circ, \beta_2 - \gamma_1, \alpha_1 - \gamma_2) \leq \theta \leq \min(360^\circ - \gamma_1 - \gamma_2, 180 + \alpha_1, 180 + \beta_2). \quad (2.8)$$

Furthermore, it should be highlighted that the way the two different scalene triangles are connected is important and different mechanical properties result for different connectivities.

(a) *On-axis mechanical properties*

The system discussed here is an anisotropic structure, i.e. a structure that behaves differently when loaded in different directions (Daniel & Ishai 1994). The behaviour of such structure when subjected to normal and/or shear stresses can be described using the  $(3 \times 3)$  symmetric compliance matrix  $\mathbf{S}$  having six independent terms that relate the applied stress  $\boldsymbol{\sigma}$  to the resulting strain  $\boldsymbol{\varepsilon}$  through  $\boldsymbol{\varepsilon} = \mathbf{S}\boldsymbol{\sigma}$ , where  $\mathbf{S}$  is of the form (Daniel & Ishai 1994):

$$\mathbf{S} = \begin{pmatrix} \frac{1}{E_1} & -\frac{\nu_{21}}{E_2} & \frac{\eta_{31}}{G_{12}} \\ -\frac{\nu_{12}}{E_1} & \frac{1}{E_2} & \frac{\eta_{32}}{G_{12}} \\ \frac{\eta_{13}}{E_1} & \frac{\eta_{23}}{E_2} & \frac{1}{G_{12}} \end{pmatrix}, \quad (2.9)$$

where  $E_i$  is the Young's modulus in the  $Ox_i$  direction,  $G_{12}$  is the shear modulus in the  $Ox_1$ - $Ox_2$  plane, whereas  $\eta_{i3}$  and  $\eta_{3i}$  are the shear coupling coefficients as defined and used elsewhere (Grima & Gatt 2010). In the case of an isotropic material, i.e. a material that has an infinite number of symmetric planes, the mechanical properties for loading at different directions are equal such that the compliance matrix reduces to

$$\mathbf{S} = \frac{1}{E} \begin{pmatrix} 1 & 1 & 0 \\ 1 & 1 & 0 \\ 0 & 0 & 0 \end{pmatrix} \quad (2.10)$$

(i) *On-axis strains*

Applying infinitesimally small stresses results in infinitesimally small changes  $d\theta$  in the angle  $\theta$  between the triangles, which in turn results in infinitesimally small uniaxial strains  $d\varepsilon_i$  in the  $Ox_i$  directions and/or infinitesimally small shear strains  $d\gamma$  in the  $Ox_{12}$  plane. These strains may be defined as

$$d\varepsilon_i = \frac{dX_{ii}}{X_{ii}} = \frac{1}{X_{ii}} \frac{dX_{ii}}{d\theta} d\theta \quad (i = 1, 2) \quad (2.11)$$

and (Grima *et al.* 2007*b*, 2010)

$$d\gamma = \frac{1}{X_{11}} \left( \cos \alpha_{12} \frac{dl_1}{d\theta} - l_1 \sin \alpha_{12} \frac{d\alpha_{12}}{d\theta} - \mu \frac{db_2}{d\theta} \right) d\theta, \quad (2.12)$$

where

$$\mu = \frac{l_1 \cos \alpha_{12}}{l_2} \quad (2.13)$$

that is

$$d\varepsilon_1 = \frac{1}{4l_2^4 X_{11}^2} \left( \begin{array}{l} 2a_1 a_2 l_2^2 (l_1^2 + l_2^2 - l_3^2) \sin(\theta + \gamma_1) \\ + b_1 b_2 (l_1^2 + l_2^2 - l_3^2) (l_1^2 - l_2^2 - l_3^2) \sin(\theta + \gamma_2) \\ + 2c_1 c_2 l_2^2 (l_1^2 - l_2^2 - l_3^2) \sin(\theta - \alpha_1 - \beta_2) \end{array} \right) d\theta \quad (2.14)$$

$$d\varepsilon_2 = \frac{dX_{22}}{X_{22}} = \frac{1}{l_2^2} b_1 b_2 \sin(\theta + \gamma_2) d\theta \quad (2.15)$$

and 
$$d\gamma = -X_{11}^{-1} l_2^{-3} (a_1 a_2 l_2^2 \sin(\theta + \gamma_1) + b_1 b_2 (l_1^2 - l_3^2) \sin(\theta + \gamma_2) + c_1 c_2 l_2^2 \sin(\theta - \alpha_1 - \beta_2)) d\theta \quad (2.16)$$

(ii) *On-axis Poisson's ratios and the shear coupling coefficients*

The Poisson's ratios  $\nu_{ij}$  in the  $Ox_i$ - $Ox_j$  plane for loading in the  $Ox_i$  direction can be defined by

$$\nu_{ij} = -\frac{d\varepsilon_j}{d\varepsilon_i} (i, j = 1, 2) \quad (2.17)$$

i.e. by substituting equations (2.14) and (2.15) in equation (2.17), the Poisson's ratios for loading in the  $Ox_i$  directions are given by

$$\begin{aligned} \nu_{21} = \nu_{12}^{-1} = & - \left( \begin{array}{l} 2a_1 a_2 l_2^2 (l_1^2 + l_2^2 - l_3^2) \sin(\theta + \gamma_1) \\ + b_1 b_2 (l_1^2 + l_2^2 - l_3^2) (l_1^2 - l_2^2 - l_3^2) \sin(\theta + \gamma_2) \\ + 2c_1 c_2 l_2^2 (l_1^2 - l_2^2 - l_3^2) \sin(\theta - \alpha_1 - \beta_2) \end{array} \right) \\ & \times (4X_{11}^2 l_2^2 b_1 b_2 \sin(\theta + \gamma_2))^{-1} \end{aligned} \quad (2.18)$$

Note that this expression may in general assume both positive and negative values as illustrated in figure 3, which shows the variation of  $\nu_{21}$  against  $\theta$  for the system in figure 2, which corresponds to a system having dimensions  $[a_1 \times b_1 \times c_1, a_2 \times b_2 \times c_2] = [2 \times 7 \times 6, 8 \times 5 \times 4]$ . In figure 3*b*, it should be noted that at  $\theta = 0^\circ$ , the structure is fully closed such that when the structure is loaded, a more open structure results owing to an expansion in both the loading and lateral directions. Such behaviour is particularly evident for space-filling structures, which will be discussed later. (electronic supplementary material, Anim-2 and Anim-6i-6xi show this more clearly.) This plot clearly shows that there are two values of  $\theta$  where the Poisson's ratio changes sign, which correspond to the values of  $\theta$  where the numerator or the denominator of the expression in equation (2.18) become zero. It should however be highlighted that this is

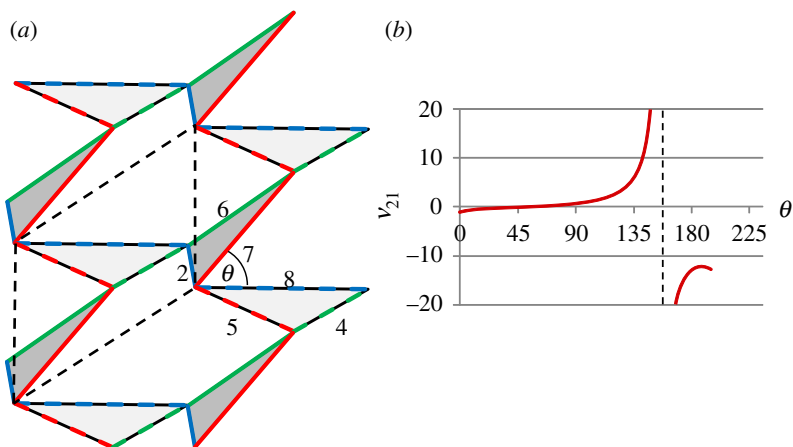


Figure 3. (a) A typical structure and (b) plot of the on-axis Poisson's ratio for a general case where  $[a_1 \times b_1 \times c_1, a_2 \times b_2 \times c_2] = [2 \times 7 \times 6, 8 \times 5 \times 4]$ . This system is geometrically realizable for hinging angle  $\theta$  between  $0^\circ$  and  $195^\circ$  (correct to nearest degree) and may be both auxetic and conventional depending on value of angle between the triangles as evident from the plot. (Online version in colour.)

not always the case. For example, as discussed below, there are some special cases where the Poisson's ratio is constant throughout the deformation with a removable discontinuity in the Poisson's ratio corresponding to a value of  $\theta$  which makes both the denominator and numerator equal to zero.

In a similar manner, the shear coupling coefficients, defined as the ratio of the normal to shear strain, are defined by

$$\eta_{13} = \eta_{31}^{-1} = \frac{d\gamma}{d\varepsilon_1} \quad \text{and} \quad \eta_{23} = \eta_{32}^{-1} = \frac{d\gamma}{d\varepsilon_2}, \quad (2.19)$$

where  $d\varepsilon_1$ ,  $d\varepsilon_2$  and  $d\gamma$  are given in equations (2.14)–(2.16). Note that, in general, these terms may be non-zero meaning that the system may shear upon uniaxial on-axis loading in the  $Ox_i$  directions.

### (iii) On-axis Young's and shear moduli

As noted above, the triangles in the structure are interconnected at their vertices through simple flexible hinges. In particular, referring to figure 1, each unit cell contains three hinges that correspond to each of the  $\varphi$ ,  $\omega$  and  $\theta$  angles (henceforth referred to as the  $\varphi$ -,  $\omega$ - and  $\theta$ -hinge, respectively), where the values of the angles  $\varphi$ ,  $\omega$  and  $\theta$  are related to each other using equation (2.1). The stiffness of the structure is imparted through the stiffness of these hinges and may be defined through a stiffness constant  $K_h$ .

The Young's moduli can be obtained by an energy conservation approach. Assuming that the only mode of deformation is hinging, i.e. the triangles are perfectly rigid, a stress applied along one of the  $Ox_i$  directions will result in a

change in the hinging angles  $\varphi$ ,  $\omega$ ,  $\theta$  denoted by  $d\varphi$ ,  $d\omega$  and  $d\theta$ , respectively. The work required to produce these changes is given by

$$W = \frac{1}{2}K_h(d\theta)^2 + \frac{1}{2}K_h(d\phi)^2 + \frac{1}{2}K_h(d\omega)^2, \quad (2.20)$$

where  $K_h$  is the stiffness constant of the hinges. Analysis of equation (2.1) implies that the changes in the hinging angles are equal to each other, i.e.  $d\theta = d\phi = d\omega$ . Thus, the total work performed per unit cell,  $W$ , is given by

$$W = \frac{3}{2}K_h(d\theta)^2. \quad (2.21)$$

The strain energy  $U$  per unit volume owing to an infinitesimally small strain  $d\varepsilon_i$  in the  $Ox_1$  direction by is defined

$$U = \frac{1}{2}E_i(d\varepsilon_i)^2, \quad (2.22)$$

where  $E_i$  is the Young's modulus of the structure along the  $Ox_i$  direction. From the principle of conservation of energy,  $U$  and  $W$  are related to each other through

$$U = \frac{W}{V}, \quad (2.23)$$

where  $V$  is the volume of the unit cell given by

$$V = X_{11}X_{22}z = \frac{z}{2}\sqrt{4l_1^2l_2^2 - (l_1^2 + l_2^2 - l_3^2)^2} \quad (2.24)$$

and  $z$  is the out-of-plane thickness of the triangles. Hence, from equations (2.14), (2.15), (2.21)–(2.24), the Young's moduli in the  $Ox_i$  direction simplify to

$$E_1 = \frac{48K_h l_2^7 X_{11}^3}{z} \left( \begin{array}{l} 2a_1 a_2 l_2^2 (l_1^2 + l_2^2 - l_3^2) \sin(\theta + \gamma_1) \\ + b_1 b_2 (l_1^2 + l_2^2 - l_3^2) (l_1^2 - l_2^2 - l_3^2) \sin(\theta + \gamma_2) \\ + 2c_1 c_2 l_2^2 (l_1^2 - l_2^2 - l_3^2) \sin(\theta - \alpha_1 - \beta_2) \end{array} \right)^{-2} \quad (2.25)$$

and

$$E_2 = \frac{3K_h l_2^3}{b_1^2 b_2^2 X_{11} z \sin^2(\theta + \gamma_2)}. \quad (2.26)$$

Through a similar energy conservation approach, the shear modulus  $G_{12}$  can be derived. In this case, the strain energy per unit volume is given by

$$U = \frac{1}{2}G_{12}(d\gamma)^2. \quad (2.27)$$

Hence, by substituting equations (2.16), (2.21) and (2.23) in equation (2.27) and re-arranging, the shear modulus simplifies to

$$G_{12} = \frac{3K_h l_2^5 X_{11}}{z} (a_1 a_2 l_2^2 \sin(\theta + \gamma_1) + b_1 b_2 (l_1^2 - l_3^2) \sin(\theta + \gamma_2) + c_1 c_2 l_2^2 \sin(\theta - \alpha_1 - \beta_2))^{-2} \quad (2.28)$$

### (b) Off-axis mechanical properties

The mechanical properties for loading in an off-axis direction may be obtained by transforming the on-axis properties using standard axis transformation techniques (Nye 1957). It should be noted that in addition to the dependency of

the Poisson's ratio and other properties on the hinging angle  $\theta$  and the lengths of the sides, the Poisson's ratio and other mechanical properties may also be dependent on the loading direction.

In particular, the Poisson's ratio of a structure made of two non-equivalent scalene triangles when loaded at angle  $\xi$  clockwise with the  $Ox_1$  axis is given by (Nye 1957)

$$\begin{aligned} \nu_{12}^{\xi} = & \left[ \frac{\nu_{12} \cos^4(\xi)}{E_1} - \cos^3(\xi) \sin(\xi) \left( \frac{\eta_{32}}{G_{12}} - \frac{\eta_{13}}{E_1} \right) \right. \\ & - \cos^2(\xi) \sin^2(\xi) \left( \frac{1}{E_1} + \frac{1}{E_2} - \frac{1}{G_{12}} \right) \\ & \left. - \cos(\xi) \sin^3(\xi) \left( \frac{\eta_{31}}{G_{12}} - \frac{\eta_{23}}{E_2} \right) + \frac{\nu_{21} \sin^4(\xi)}{E_2} \right] E_1^{\xi}, \end{aligned} \quad (2.29)$$

where

$$\begin{aligned} E_1^{\xi} = & \left[ \frac{\cos^4(\xi)}{E_1} + \cos^3(\xi) \sin(\xi) \left( \frac{\eta_{31}}{G_{12}} + \frac{\eta_{13}}{E_1} \right) \right. \\ & - \cos^2(\xi) \sin^2(\xi) \left( \frac{\nu_{12}}{E_1} + \frac{\nu_{21}}{E_2} - \frac{1}{G_{12}} \right) \\ & \left. + \cos(\xi) \sin^3(\xi) \left( \frac{\eta_{23}}{E_2} + \frac{\eta_{32}}{G_{12}} \right) + \frac{\sin^4(\xi)}{E_2} \right]^{-1}. \end{aligned} \quad (2.30)$$

The off-axis plots that correspond to the systems illustrated in figure 2 (i.e. the structure  $[2 \times 7 \times 6, 8 \times 5 \times 4]$  when  $\theta = 50^\circ, 100^\circ$  and  $150^\circ$ ) are shown in figure 4. Note that as already pointed out when discussing the on-axis Poisson's ratio, in general the structure may be auxetic and non-auxetic for loading at different off-axis angle  $\xi$ , i.e. the Poisson's ratio depends not only on the geometric parameters (i.e. the lengths of sides of the triangles and the hinging angle  $\theta$ ) but also on the loading direction  $\xi$ . However, this is not always the case and as discussed below, for example, the system where  $a_1 = b_1 = c_1 = a_2 = b_2 = c_2$  has a constant Poisson's value of  $-1$ , which is independent of the loading direction (Grima & Evans 2006). Note also that there seems to be no apparent correlation between the direction at which maximum auxeticity is obtained and the geometry of the structure. This can be inferred by comparing the polar plots of the off-axis Poisson's ratio  $\nu_{12}^{\xi}$  against the loading direction  $\xi$  in figure 4 with the structures at the corresponding hinging angle shown in figure 2, and that there may be particular systems that are not auxetic for loading in any direction.

### 3. Discussion

The expressions and plots presented above highlight the fact that systems made from rigid triangular units that can rotate relative to each other may exhibit negative Poisson's ratios. This is very significant, not only due to the fact that it is well known that a negative Poisson's ratio is a highly desirable property and may lead to enhancements of various useful properties, but also in view

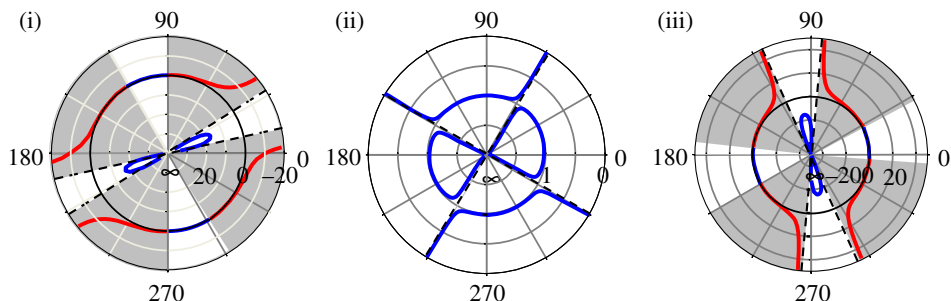


Figure 4. The off-axis Poisson's ratio for the structure discussed shown in figure 2:  $[a_1 \times b_1 \times c_1, a_2 \times b_2 \times c_2] = [2 \times 7 \times 6, 8 \times 5 \times 4]$  at hinging angles  $50^\circ$ ,  $100^\circ$ ,  $150^\circ$ . The shaded regions show ranges of loading direction where the system is auxetic. It is clearly evident that auxeticity for a particular structure depends on the hinging angles and on the loading direction. (Online version in colour.)

of the fact that as discussed below, there are various auxetic materials that have nano or microstructural features, which make them describable through the model presented here, including the (010) plane of the nepheline hydrate I (JBW) zeolite (Grima *et al.* 2000), hypothetical polyphenylacetylene networks (Grima & Evans 2000*b*) and the microstructure of foam (Grima *et al.* 2006). However, the equations also highlight the fact that not all systems made from rotating rigid triangles exhibit negative Poisson's ratios since for a given set of triangles  $[a_1 \times b_1 \times c_1, a_2 \times b_2 \times c_2]$  the occurrence or otherwise of auxetic behaviour may depend on the angle between the triangles and the direction of loading. For example, figure 3 clearly shows that for loading in the  $Ox_2$  direction, the Poisson's ratio  $\nu_{21}$  of the system in figure 2 having triangles of dimensions  $[2 \times 7 \times 6, 8 \times 5 \times 4]$  may be either negative or positive, depending on the angle between the triangles,  $\theta$ . In fact, figure 3 suggests that the Poisson's ratio  $\nu_{21}$  is negative for systems having small values of  $\theta$ , which become positive through a continuous transition when  $\theta \approx 58^\circ$ , a value that makes the numerator of equation (2.18) equal to zero and then changes sign again in an asymptotic manner when  $\theta \approx 156^\circ$ , which corresponds to the point when the denominator of equation (2.18) is equal to zero (i.e. when  $\sin(\theta + \gamma_2) = 0$ ). Note that this asymptotic change in the Poisson's ratio occurs at the point where the Young's modulus in the  $Ox_2$  direction becomes infinite ( $\sin(\theta + \gamma_2)$  is also in the denominator of  $E_2$ ), thus suggesting that the system becomes 'locked' for stretching in the  $Ox_2$  directions. This 'locking' occurs as a result of the fact that as illustrated in figure 5*a*, the system when  $\sin(\theta + \gamma_2)$  corresponds to the 'fully open' conformation of this structure in the  $Ox_2$  direction, something that happens when the side  $b_1$  becomes aligned with  $b_2$  and with the  $Ox_2$  direction (the stretching direction). Obviously, it should be noted that the systems with  $\theta$  being greater than the 'locking angle' (i.e. the angle when the structure becomes locked upon stretching) are geometrically feasible and in such systems, stretching would result in a decrease in the angle  $\theta$ , not an increase. In fact, it should be noted that one may 'force' the system to move from one side of the 'locking angle' to the other by physically rotating one of the triangles, or, if possible, by applying a moment through shearing.

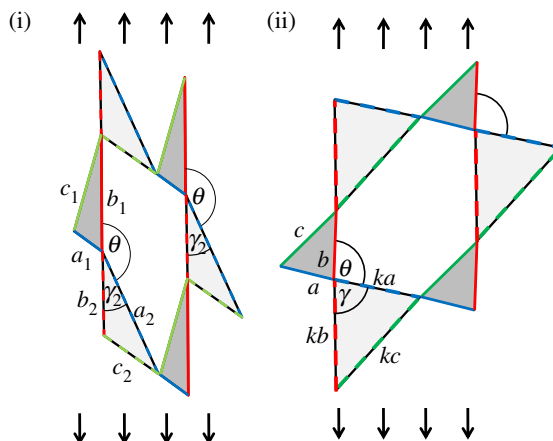


Figure 5. Structures at the ‘locking angle’: (i) an example of a general system having triangular dimensions  $[a_1 \times b_1 \times c_1, a_2 \times b_2 \times c_2] = [2 \times 7 \times 6, 8 \times 5 \times 4]$  and (ii) a particular system having triangular dimensions  $[a \times b \times c, ka \times kb \times kc] = [0.8 \times 1.0 \times 1.2, 1.6 \times 2.0 \times 2.4]$ . Locking of the structure (i) occurs when the sides of length  $b_1$  and  $b_2$  are aligned with the loading direction, i.e. when  $\theta + \gamma_2 = 180^\circ$ , in this case when  $\theta = 156^\circ$ . In the particular case (ii) where the triangles are similar, the structure is locked when sides of length  $a$ ,  $b$  and  $c$  in one triangle are aligned collinearly with sides of length  $ka$ ,  $kb$  and  $kc$  of the other triangle that geometrically explains why such system ‘lock’ at the same value of  $\theta$  ( $\theta = 180^\circ - \gamma$ ) for loading in any direction. Obviously, this will not be possible in the general case where the locking angle is dependent on the direction of loading. (Online version in colour.)

Note also that as  $\nu_{12} = \nu_{21}^{-1}$ , the continuous transition in  $\nu_{21}$  necessarily corresponds to an asymptotic transition in  $\nu_{12}$ , a point that corresponds to the point when  $E_1$  becomes infinite, i.e. the system becomes ‘locked’ for stretching in the  $Ox_1$  directions. This may be easily inferred by looking at the expressions for  $\nu_{12}$  and  $E_1$ , which share the same denominator. It should also be noted that the Poisson’s ratios  $\nu_{12}$  and  $\nu_{21}$  must necessarily have the same sign since these two properties are the reciprocal of each other.

Although the behaviour illustrated in figures 3 and 4 is typical for systems where  $a_1 \neq b_1 \neq c_1 \neq a_2 \neq b_2 \neq c_2$ , not all systems behave in this manner. In fact, as discussed in electronic supplementary material, appendix A, there are various special cases arising from particular combinations of the dimensions of the triangles in the generalized model where the behaviour is much simpler.

In particular, it is shown that the Poisson’s ratio of the congruent equilateral triangles structure, denoted by  $[a \times a \times a, a \times a \times a]$  (figure 6i), is equal to  $-1$  for all values of the hinging angle  $\theta$  and for all loading directions, i.e. its Poisson’s ratio is strain-independent and isotropic. This is in accordance with previous work by Grima & Evans (2006). Furthermore, this system does not shear upon loading since it exhibits an infinite shear modulus. It is interesting to note that such non-shearing systems having isotropic strain-independent Poisson’s ratio of  $-1$  may be obtained from the much more general system  $[a \times b \times c, ka \times kb \times kc]$  (figure 6xi), which may be regarded as the parent case of a number of much more symmetric systems. These include the system  $[a \times a \times a, ka \times ka \times ka]$ , which represents a system made from two

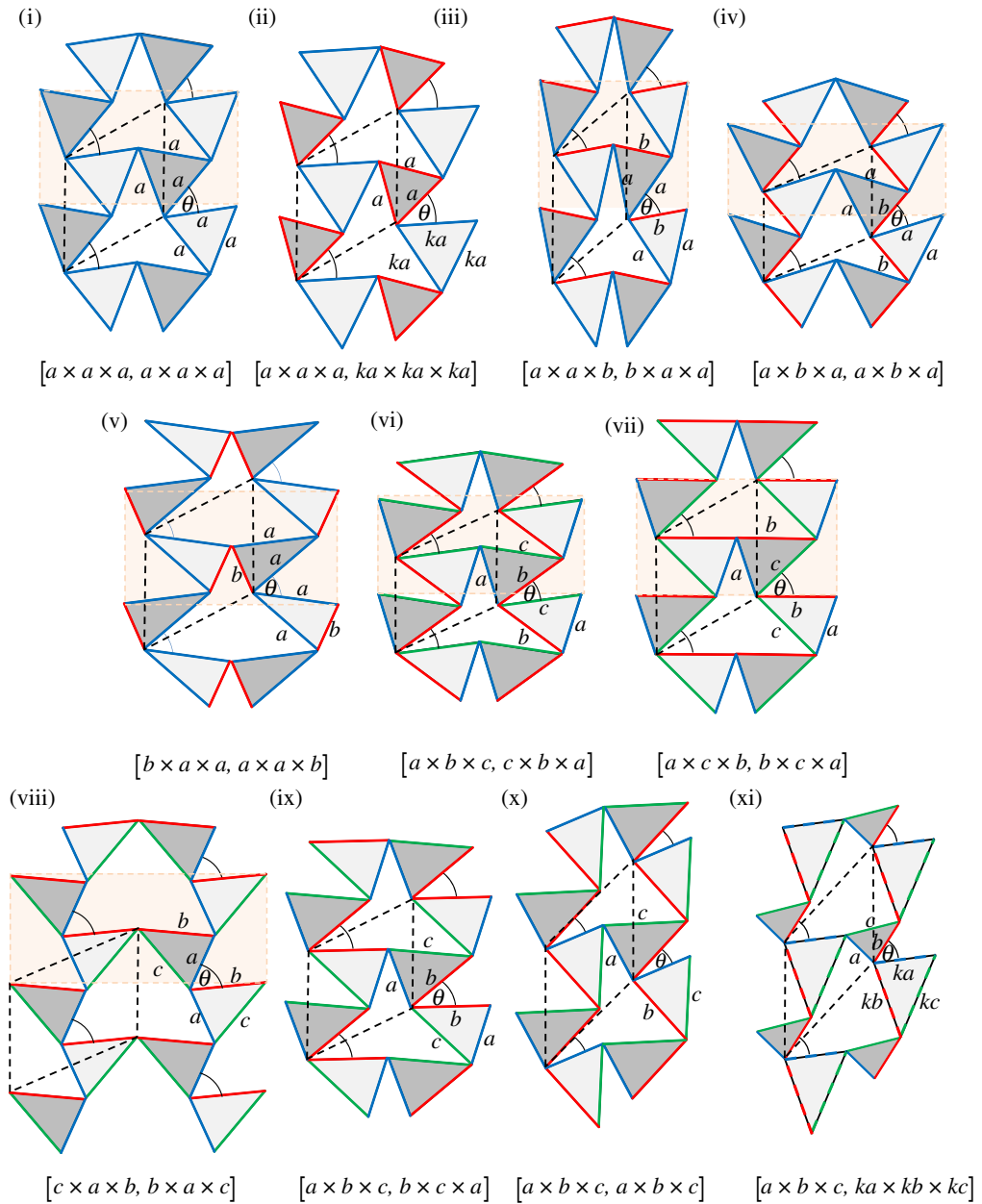


Figure 6. The special cases of the structure  $[a_1 \times b_1 \times c_1, a_2 \times b_2 \times c_2]$  considered in this work, namely (i) The congruent equilateral triangles; (ii) The different-sized equilateral triangles; (iii–v) congruent isosceles triangles; (vi–x) congruent scalene triangles; (xi) similar scalene triangles. Cases (i), (ii), (iv), (x) and (xi) are isotropic and strain-independent with Poisson's ratios of  $-1$ . As can be seen cases, (i), (iii)–(vii) can be described using a rectangular unit cell. Such structures do not shear when loaded along their line of symmetry, i.e. along  $Ox_2$ . Animations illustrate how these structures behave when uniaxial loaded are shown in electronic supplementary material, Anim-6i–6xi. These structures are discussed in detail in the electronic supplementary material, appendix A. (Online version in colour.)

similar equilateral triangles (figure 6ii); the system  $[a \times b \times a, a \times b \times a]$ , which represents one of the three systems made from congruent isosceles triangles (figure 6iv); the system  $[a \times b \times c, a \times b \times c]$ , which represents one of the systems made from congruent scalene triangles (figure 6x). It is interesting to note that in these isotropic systems, the ‘locking’ angle is equal to  $180^\circ - \gamma$  not only for loading in the  $Ox_2$  direction but also in other directions. Also, unlike what is observed in the general case, there is no asymptotic transition in the Poisson’s ratio at the locking angle, but a ‘removable discontinuity’. In fact, it should be noted that, while in general the profile of  $\nu_{21}$  against  $\theta$  has a continuous and an asymptotic transition, for these systems the numerator and denominator equation (2.18) for  $\nu_{21}$  are equal to zero for the same hinging angle and thus only a removable discontinuity at  $\theta = 180^\circ - \gamma$  results. Obviously, owing to the isotropy, this property is exhibited not only in the  $Ox_2$  direction but also in all directions. Geometrically, this locking angle corresponds to the conformation where sides of length  $a$ ,  $b$  and  $c$  in one triangle are aligned collinearly with sides of length  $ka$ ,  $kb$  and  $kc$  of the other triangle (figure 5ii).

Also of interest are systems with a line of symmetry, which can be defined using a rectangular unit cell containing four congruent triangles (as shown in figure 6), a property which clearly suggests that when such systems are loaded along this line of symmetry, no shearing takes place. Such structures include the congruent scalene cases  $[a \times b \times c, c \times b \times a]$ ,  $[a \times c \times b, b \times c \times a]$  and  $[c \times a \times b, b \times a \times c]$  (figure 6f, g, h, respectively) and some of the systems discussed above, namely the equilateral and isosceles cases  $[a \times a \times a, a \times a \times a]$  and  $[a \times a \times b, b \times a \times a]$  as discussed by Grima and co-workers (Grima & Evans 2006, Grima *et al.* 2010; figure 6i,iii, respectively) and the cases  $[a \times b \times a, a \times b \times a]$  and  $[b \times a \times a, a \times a \times b]$  (figure 6iv,v, respectively). The symmetry present in these structures is also reflected in the off-axis plots where the Poisson’s ratio obtained when loading at an angle  $\xi$  is the same as that for loading at an angle  $180^\circ - \xi$ . Furthermore, the system consisting of congruent equilateral triangles (figure 6i), congruent isosceles system  $[b \times a \times a, a \times a \times b]$  (figure 6v) and the congruent scalene system  $[a \times b \times c, b \times c \times a]$  (figure 6ix) are also space-filling when  $\theta = 0^\circ$  as can be seen in electronic supplementary material, animations 6v,vi, respectively, something that does not happen in the general case. The special cases highlighted here are discussed in more detail in the electronic supplementary material, appendix A.

Let us now discuss some situations where the models derived above may be applied in practical applications. In this respect, it should be highlighted that, in recent years, (Grima *et al.* 2006, 2009) had identified a number of auxetic or potentially auxetic real materials such as foams or zeolite materials (Grima *et al.* 2000), where the deformation mechanism leading to the negative Poisson’s ratio could be described in terms of two-dimensional rotating rigid or semi-rigid units having the shape of a triangle. For instance, it has been proposed that the zeolite JBW framework may exhibit auxetic behaviour in its (010) plane through a mechanism that may be described through a rotating triangle model (Grima *et al.* 2000). More recently, it has been proposed by Grima *et al.* (2006) that the auxeticity in auxetic foam can be explained through rotation of rigid units—in particular, rotating rigid equilateral triangles connected at their vertices. This hypothesis can be confirmed through images of the microstructure of both the conventional and the auxetic foam, which indicate that there is

additional thickness in the region where the ribs of the foam meet at a particular point (Grima *et al.* 2006). These features may result in the ‘joints’ behaving as rigid (or semi-rigid) units, which—in the auxetic foams—are oriented in such a way that permit them to rotate relative to each other to form a more open microstructure, hence the auxetic behaviour. Experimental evidence which confirms the important role that such mechanistic features have, has recently been obtained by McDonald *et al.* (2010) through three-dimensional X-ray microtomography. In fact it was shown that the rotation of rigid units has a very important role in generating the observed negative Poisson’s ratio in such foams. Furthermore, the presence of indentations in auxetic foams which act as hinges that result in rotation of the units upon loading is also evident in SEM images by Bianchi *et al.* (2010). Here, it should be emphasized that although the model presented here still needs to be further developed to permit the possibility that the triangular units themselves change shape, it offers a very significant improvement over the existing published models as all the earlier models were based on highly symmetric units. While these earlier models may have been sufficient to model the properties of idealized forms of crystalline systems, it is not surprising that the regularity of Grima’s earlier models always posed difficulty in describing real materials such as foams, which are characterized by a microstructure that is highly asymmetric and irregular. The model discussed here marks an important step forward in this respect since—for the first time—it has been made possible to predict the properties of a system that is much less regular, achieved by increasing the number of geometric parameters through the use of scalene triangles, something that would enable it to be used in a wider range of situations. In this respect, it should be noted that the model presented here can easily explain three properties of the foam: (i) the fact that Poisson’s ratio in the auxetic foams need not be  $-1$ , (ii) the fact that foams in particular auxetic foams are anisotropic as evident in the results obtained by Bianchi *et al.* (2011) and (iii) the fact that foams that are auxetic at low strains may start to exhibit conventional positive Poisson’s ratios at higher strains. Note that the latter can be deduced from figure 3*b* which shows that as the structure is loaded and the hinging angle increases (up to the locking position), the Poisson’s ratio value changes from negative to positive. Furthermore, the model presented here can be used to predict the variation in the surface density (the two-dimensional equivalent of the normal volumetric density) or the relative surface density of foam (i.e. the two-dimensional equivalent of the normal volumetric density divided by the density of the undeformed foam). The suitability of our model to predict such density variations is clearly illustrated in figure 7, which shows how the predictions from our model compare with the experimental results on auxetic polyurethane foams obtained by Smith *et al.* (2000). (Details on the calculations involved in comparing the relative surface density as a function of true strain obtained analytically and through experiments are given in the electronic supplementary material, appendix A.)

Before proceeding any further, it should be highlighted that knowledge of which structural features and mechanistic deformation is responsible for the observed mechanical properties is important not only because it helps us understand better the relationship between the microstructure and the macroproperties of the material but also because it can help us predict how the material will behave in particular practical applications. One such application is that of filtration,

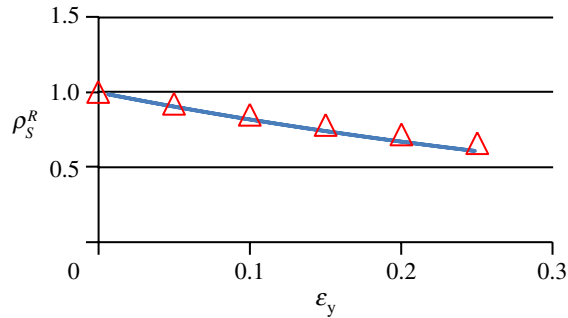


Figure 7. Plot of relative surface density against true strain in the loading direction  $Ox_2$  obtained analytically (solid line) where the structure is made of unit cells denoted by  $[a_1 \times b_1 \times c_1, a_2 \times b_2 \times c_2]$  with the sides  $[37.5 \times 22.5 \times 37.5, 37.5 \times 22.5 \times 37.5]$  (in millimetres) and experimentally (data points) using the data obtained by Smith *et al.* (2000). The methodology used for obtaining this comparison is discussed in electronic supplementary material, appendix A. Note the excellent agreement between the experimental data published by Smith *et al.* (2000) and the model proposed here, thus highlighting the adequacy of this model to predict the behaviour of foam. (Online version in colour.)

which generally involves the use of micro or nanostructured materials and where it was recently proved that a negative Poisson's ratio may impart several beneficial properties on filters (Alderson *et al.* 2000; Rasburn *et al.* 2001). In particular, unlike conventional filters that have limited pore tunability properties and tend to become easily clogged, auxetic filters can easily be cleaned simply by applying a stress that opens the pore size further to facilitate filter cleaning. Other practical advantages afforded by auxetic filter include the ability to store particular substances within their pores, which may then be easily released when needed through the application of a mechanical stress. This feature may make auxetics suitable for use in a wide range of scenarios ranging from fuel storage applications to medical applications where auxetics are used as smart bandages, which can release medication on demand in a controlled manner (Alderson & Alderson 2007).

In addition, models such as those derived here are of particular use to researchers and industrialists who are working on designing and developing new materials, with tailor-made properties for use in particular practical applications. The model proposed here is characterized by its ability to offer a very wide range of mechanical properties, which may be fine-tuned through the choice of the geometric properties associated with the triangles. Given the current state of the art, one interesting application of the proposed model would be the possibility of using it as the underlying knitted geometry in auxetic textiles in analogy with the previous work by Hu *et al.* (2010), where the rotating squares structure was used. Also, this model can provide experimentalists with a 'blueprint' for the manufacture of auxetics by including perforations of the right shape and position so that the resulting system may behave in a manner similar to that predicted by this model. Modelling and experimental work on such systems have already confirmed that this principle can indeed result in auxetic behaviour (Bertoldi *et al.* 2010; Grima & Gatt 2010; Grima *et al.* 2010) and the additional variability associated with the current model will make it possible to achieve a higher degree of tunability of the properties afforded by such systems.

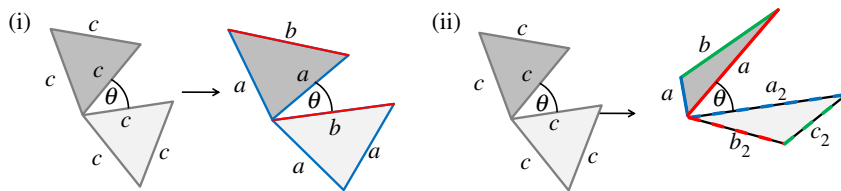


Figure 8. The structure made of congruent equilateral triangles subjected to heat energy results in a different-sized triangle depending on the amount of different thermal coefficients that the structure has. This results in a change in the Poisson's ratio of the triangle from a Poisson's ratio of  $-1$  to a Poisson's ratio that is dependent on the new lengths of the sides of the triangles and the hinging angle. The new structures obtained when the structure is subjected to heating if (i) all sides have one of two different thermal coefficients and (ii) all sides have a different thermal coefficient are presented. (Online version in colour.)

Finally, it should be noted that the model presented here may be easily adapted so as to produce a template for the design of auxetics where the degree of auxeticity can be temperature-dependent. Such property may be achieved if the triangles are constructed in a truss-like manner from beam elements having different thermal expansion coefficients. If such systems experience a change in temperature, then there will be an uneven extent of expansion in the side lengths of the triangles with the result that the triangles change shape and hence the system will exhibit different mechanical properties. To illustrate this concept, one may look at a structure which—at a temperature  $T_0$ —is made of congruent equilateral triangles. As illustrated in figure 8i, if the triangles in such structure are made in such a way that one of their sides is made from a material that responds more to heat than the other sides, then a change in temperature from  $T_0$  to  $T_0 + \Delta T$  will cause the triangle to deform to isosceles triangles, which system will have different Poisson's ratios than the system at a temperature  $T_0$ . Here, it should be highlighted that the model presented here suggests that the macroscopic Poisson's ratio properties of such systems would depend on which of the sides is made to have different thermal properties from the others since there are different ways that isosceles triangles can be connected (figure 6iii–v). Obviously, the model discussed here caters for even more complex structures whereby both triangles have sides with different thermal expansion coefficients, resulting in a system with six sides that behave differently to temperature (figure 8b). For such systems, the on-axis Poisson's ratio, Young's and shear moduli at a temperature  $T$  are given by the equations derived above (equations (2.18), (2.25), (2.26), (2.28)), which are modified so that the side lengths are made functions of temperatures, for example, through expressions such as

$$l = l_0[1 + \alpha_L(T - T_0)], \quad (3.1)$$

where  $l$  is the length of the particular side at a temperature  $T$ ,  $l_0$  is its respective length at a reference temperature  $T_0$  and  $\alpha_L$  is its linear coefficient of thermal expansion.

Before concluding it is important to note that although the model presented here is highly generic and can be used in a wide range of applications, it still has some limitations which may need to be addressed in the future. In particular,

the model presented here is a two-dimensional model while real materials are characterized with nano and microstructures that are of a three-dimensional nature. In such cases, the model presented here may only be used to explain the behaviour in one particular plane of the material. Although previous work in this field has confirmed that such an approach still yields highly valuable information on the behaviour of real materials (Grima *et al.* 2000, 2005; Alderson & Evans 2002), any deformations that result as a consequence of the three-dimensional nature of the micro or nanostructure will not be adequately represented in this model. Furthermore, the model presented was based on the assumption that the triangular units remain perfectly rigid throughout the deformation process. Such idealized behaviour is unlikely to be observed in real materials where the rotation of the units will probably be accompanied by a simultaneous change in the shape of the units, possibly owing to stretching of the sides, i.e. the units are semi-rigid rather than fully-rigid. Such change in shape may cause drastic changes in the mechanical properties, for example, a structure that, due to being of the type  $[a \times b \times c, ka \times kb \times kc]$ , was isotropic with a Poisson's ratio of  $-1$  will cease to be isotropic if the sides of a particular triangle do not change length in proportion to each other, hence resulting in non-similar triangles. Similar effects were observed in the rotating squares model when the constraint of perfectly rigid squares was relaxed (Grima *et al.* 2007c; Attard *et al.* 2009). Probably more important is the fact that non-crystalline materials such as foams may be significantly more irregular than what is permitted through the model presented here. The extension of the model presented here to incorporate such features is likely to further extend the suitability of this model to explain and predict the mechanical behaviour of real materials.

#### 4. Conclusion

In this work, the mechanical properties of a highly generic model structure made up of two different scalene triangles have been derived and discussed. Analysis of this model confirms that auxetic behaviour may be obtained from such systems, the extent of which is dependent on the shape of the triangles and the way they are connected together. For example, it was shown that some structures—in particular, all structures made of two similar triangles denoted by  $[a \times b \times c, ka \times kb \times kc]$ —are isotropic with a Poisson's ratio of  $-1$  while other structures have a Poisson's ratio dependent on the length of sides of triangles, on the hinging angle between the triangles and on the loading direction. It was also shown that this model can be used to explain auxeticity in various classes of materials. For example, an analogy between this model and the microstructure of foam was highlighted, eliciting the significance of this work in the study of auxetic foam materials behaviour, including the prediction of the dependency of density with strain. Given the various enhanced properties of auxetic structures, it is hoped that this model will stimulate further work, which could lead to better understanding of naturally occurring and man-made auxetics and present systems and possibly to the manufacture of new auxetic systems that mimic the behaviour of the model presented here.

The authors gratefully acknowledge the support of Malta Council for Science and Technology.

## References

- Alderson, A. 1999 A triumph of lateral thought. *Chem. Ind.* **384**, 384–391.
- Alderson, A. & Alderson, K. L. 2007 Auxetic materials. *Proc. Inst. Mech. Eng. G J. Aerosp.* **221**, 565–575. (doi:10.1243/09544100JAERO185)
- Alderson, A. & Evans, K. E. 2002 Molecular origin of auxetic behaviour in tetrahedral framework silicates. *Phys. Rev. Lett.* **89**, 225 503–225 507. (doi:10.1103/PhysRevLett.89.225503)
- Alderson, K. L., Alderson, A. & Evans, K. E. 1997 The interpretation of the strain-dependent Poisson's ratio in auxetic polyethylene. *J. Strain Anal. Eng. Des.* **32**, 201–212. (doi:10.1243/0309324971513346)
- Alderson, A., Rasburn, J., Ameer-Beg, S., Mullarkey, P. G., Perrie, W. & Evans, K. E. 2000 An auxetic filter: a tuneable filter displaying enhanced size selectivity or de-fouling properties. *Ind. Eng. Chem. Res.* **39**, 654–665. (doi:10.1021/ie990572w)
- Alderson, A., Alderson, K. L., Evans, K. E., Grima, J. N., Williams, M. R. & Davies, P. J. 2005 Modelling the deformation mechanisms, structure–property relationships and applications of auxetic nanomaterials. *Phys. Status Solid B* **242**, 499–508. (doi:10.1002/pssb.200460370)
- Ashby, M. F., Gibson, L. J., Wegst, U. & Olive, R. 1995 The mechanical properties of natural materials I. material property charts. *Proc. R. Soc. Lond. A* **450**, 123–140. (doi:10.1098/rspa.1995.0075)
- Attard, D., Manicaro, E., Gatt, R. & Grima, J. N. 2009 On the properties of auxetic rotating stretching squares. *Phys. Status Solid B* **246**, 2045–2054. (doi:10.1002/pssb.200982035)
- Baughman, R. H., Shacklette, J. M., Zakhidov, A. A. & Stafstrom, S. 1998 Negative Poisson's ratios as a common feature of cubic metals. *Nature* **392**, 362–365. (doi:10.1038/32842)
- Bertoldi, K., Reis, P. M., Willshaw, S. & Mullin, T. 2010 Negative Poisson's ratio behaviour induced by an elastic instability. *Adv. Mater.* **22**, 361–366. (doi:10.1002/adma.200901956)
- Bezazi, A. & Scarpa, F. 2006 Mechanical behaviour of conventional and negative Poisson's ratio thermoplastic polyurethane foams under compressive cyclic loading. *Int. J. Fatigue* **29**, 922–930. (doi:10.1016/j.ijfatigue.2006.07.015)
- Bianchi, M., Scarpa, F. & Smith, C. W. 2010 Shape memory behaviour in auxetic foams: mechanical properties. *Acta Mater.* **58**, 858–865.
- Bianchi, M., Scarpa, F., Banse, M. & Smith, C. W. 2011 Novel generation of auxetic open cell foams for curved and arbitrary shapes. *Acta Mater.* **59**, 686–691. (doi:10.1016/j.actamat.2010.10.006)
- Burke, M. 1997 A stretch of the imagination. *New Sci.* **154**, 36–39.
- Chan, N. & Evans, K. E. 1997 Fabrication methods for auxetic foams. *J. Mater. Sci.* **32**, 5945–5953. (doi:10.1023/A:1018606926094)
- Choi, J. B. & Lakes, R. S. 1995 Nonlinear analysis of the Poisson's ratio of negative Poisson's ratio foams. *J. Compos. Mater.* **29**, 113–128. (doi:10.1177/002199839502900106)
- Daniel, I. M. & Ishai, O. 1994 *Engineering mechanics of composite materials*. New York, NY: Oxford University Press.
- EPSRC: Engineering and Physical Sciences Research Council. 2010 *Expanding blast-proof curtain will reduce impact of bomb explosions*. Public release date: 21 June 2010. EPSRC Press Office. See <http://www.epsrc.ac.uk/newsevents/news/2010/Pages/blastproofcurtain.aspx>.
- Evans, K. E. 1991 Auxetic polymers: a new range of materials. *Endeavor* **15**, 170–174. (doi:10.1016/0160-9327(91)90123-S)
- Evans, K. E. & Caddock, B. D. 1989 Microporous materials with negative Poisson's ratios. II. Mechanisms and interpretation. *J. Phys. D Appl. Phys.* **22**, 1883–1887. (doi:10.1088/0022-3727/22/12/013)
- Evans, K. E., Nkansah, M. A., Hutchinson, I. J. 1994 Auxetic foams: modelling negative Poisson ratios. *Acta Mater.* **42**, 1289–1294. (doi:10.1016/0956-7151(94)90145-7)
- Gibson, L. J., Ashby, M. F., Schajer, G. S. & Robertson, C. I. 1982 The mechanics of two-dimensional cellular materials. *Proc. R. Soc. Lond. A* **382**, 25–42. (doi:10.1098/rspa.1982.0087)
- Gibson, L. J., Ashby, M. F., Karam, G. N., Wegst, U., Shercliff, H. R. 1995 The mechanical properties of natural materials II: microstructures for mechanical efficiency. *Proc. R. Soc. Lond. A* **450**, 141–162. (doi:10.1098/rspa.1995.0076)

- Grima, J. N. & Evans, K. E. 2000a Auxetic behaviour from rotating squares. *J. Mater. Sci. Lett.* **19**, 1563–1565. (doi:10.1023/A:1006781224002)
- Grima, J. N. & Evans, K. E. 2000b Self expanding molecular networks. *Chem. Commun.* **16**, 1531–1532. (doi:10.1039/B004305M)
- Grima, J. N. & Evans, K. E. 2006 Auxetic behaviour from rotating triangles. *J. Mater. Sci.* **41**, 3193–3196. (doi:10.1007/s10853-006-6339-8)
- Grima, J. N. & Gatt, R. 2010 Perforated sheets exhibiting negative Poisson's ratios. *Adv. Eng. Mater.* **12**, 460–464. (doi:10.1002/adem.201000005)
- Grima, J. N., Jackson, R., Alderson, A. & Evans, K. E. 2000 Do zeolites have negative Poisson's ratios? *Adv. Mater.* **12**, 1912–1918. (doi:10.1002/1521-4095(200012)12:24<1912::AID-ADMA1912>3.0.CO;2-7)
- Grima, J. N., Gatt, R., Alderson, A. & Evans, K. E. 2005 On the origin of auxetic behaviour in the silicate  $\alpha$ -cristobalite. *J. Mater. Chem.* **15**, 4003–4005. (doi:10.1039/b508098c)
- Grima, J. N., Gatt, R., Ravirala, N., Alderson, A. & Evans, K. E. 2006 Negative Poisson's ratios in cellular foam materials. *Mat. Sci. Eng. A* **423**, 214–218. (doi:10.1016/j.msea.2005.08.229)
- Grima, J. N., Gatt, R., Zammit, V., Williams, J. J., Evans, K. E., Alderson, A. & Walton, R. I. 2007a Natrolite: a zeolite with negative Poisson's ratios. *J. Appl. Phys.* **101**, 86 102–86 105. (doi:10.1063/1.2718879)
- Grima, J. N., Farrugia, P. S., Gatt, R. & Zammit, V. 2007b A system with adjustable positive or negative thermal expansion. *Proc. R. Soc. A* **463**, 1585–1596. (doi:10.1098/rspa.2007.1841)
- Grima, J. N., Zammit, V., Gatt, R., Alderson, A. & Evans, K. E. 2007c Auxetic behaviour from rotating semi-rigid units. *Phys. Status Solidi B* **244**, 866–882. (doi:10.1002/pssb.200572706)
- Grima, J. N., Farrugia, P. S., Caruana, C., Gatt, R. & Attard, D. 2008a Auxetic behaviour from stretching connected squares. *J. Mater. Sci.* **43**, 5962–5971. (doi:10.1007/s10853-008-2765-0)
- Grima, J. N., Gatt, R., Farrugia, P. S. 2008b On the properties of auxetic meta-tetrachiral structures. *Phys. Status Solidi B* **245**, 511–520. (doi:10.1002/pssb.200777704)
- Grima, J. N., Attard, D., Gatt, R., Cassar, R. N. 2009 A novel process for the manufacture of auxetic foams and their reversion to conventional form. *Adv. Eng. Mater.* **11**, 533–535. (doi:10.1002/adem.200800388)
- Grima, J. N., Gatt, R., Ellul, B., Chetcuti, E. 2010 Auxetic behaviour in non-crystalline materials having star or triangular shaped perforations. *J. Non-Cryst Solids* **356**, 1980–1987. (doi:10.1016/j.jnoncrysol.2010.05.074)
- Grima, J. N., Manicaro, E. & Attard, D. 2011 Auxetic behaviour from connected different-sized squares and rectangles. *Proc. R. Soc. A* **467**, 439–458. (doi:10.1098/rspa.2010.0171)
- He, C. B., Liu, P. W. & Griffin, A. C. 1998 Toward negative Poisson ratio polymers through molecular design. *Macromolecules* **31**, 3145–3147. (doi:10.1021/ma970787m)
- Hook, P. B., Evans, K. E., Hannington, J. P., Hartmann-Thompson, C. & Bunce, T. R. 2006 *Snapping fabrics* KR20060009826.
- Hu, H., Wang, Z., Liu, S. & Liu, Y. 2010 Development of Auxetic fabrics using flat knitting technology. *Textile Res. J.* **81**, 1493–1502. (doi:10.1177/0040517511404594)
- Ishibashi, Y. & Iwata, M. 2000 A microscopic model of a negative Poisson's ratio in some crystals. *J. Phys. Soc. Jpn.* **69**, 2702–2703. (doi:10.1143/JPSJ.69.2702)
- Lakes, R. S. 1987 Foam structures with a negative Poisson's ratio. *Science* **235**, 1038–1040. (doi:10.1126/science.235.4792.1038)
- Lakes, R. S. 1991 Deformation mechanisms of negative Poisson's ratio materials: structural aspects. *J. Mater. Sci.* **26**, 2287–2292. (doi:10.1007/BF01130170)
- Lakes, R. S. & Elms, K. E. 1993 Indentability of conventional and negative Poisson's ratio foams. *J. Compos. Mater.* **27**, 1193–1202. (doi:10.1177/002199839302701203)
- Lees, C., Vincent, J. F. V. & Hillerton, J. E. 1991 Poisson's ratio in skin. *Biomed. Mater. Eng.* **1**, 19–23.
- Liu, Y., Hu, H., Lam, J. K. C. & Liu, S. 2010 Negative Poisson's ratio weft-knitted fabrics. *Tex. Res. J.* **80**, 856–863. (doi:10.1177/0040517509349788)
- Masters, I. G. & Evans, K. E. 1996 Models for the elastic deformation of honeycombs. *Compos. Struct.* **35**, 403–422. (doi:10.1016/S0263-8223(96)00054-2)

- McDonald, S. A., Dedreuil-Monet, G., Yao, Y. T., Alderson, A. & Withers, P. J. 2010 *In situ* 3D X-ray microtomography study comparing auxetic and non-auxetic polymeric foams under tension. *Phys. Status Solidi B* **248**, 45–51. (doi:10.1002/pssb.201083975)
- Nye, J. F. 1957 *Physical properties of crystals*, pp. 33–49. New York, NY: Oxford University Press.
- Rasburn, J., Mullarkey, P. G., Evans, K. E., Alderson, A., Ameer-Beg, S., Perrie, W. 2001 Auxetic structures for variable permeability systems. *AIChE J.* **47**, 2623–2626. (doi:10.1002/aic.690471125)
- Scarpa, F. & Smith, F. C. 2004 Passive and MR fluid-coated auxetic PU foam—mechanical, acoustic, and electromagnetic properties. *J. Intell. Mater. Syst. Struct.* **15**, 973–979. (doi:10.1177/1045389X04046610)
- Scarpa, F. & Tomlinson, G. 2000 Theoretical characteristics of the vibration of sandwich plates with in-plane negative Poisson's ratio values. *J. Sound Vib.* **230**, 45–67. (doi:10.1006/jsvi.1999.2600)
- Scarpa, F., Bullough, W. A. & Lumley, P. 2004 Trends in acoustic properties of iron particle seeded auxetic polyurethane foam. *Proc. Inst. Mech. Eng. C J. Mech. Eng. Sci.* **218**, 241–244. (doi:10.1243/095440604322887099)
- Smith, C. W., Grima, J. N. & Evans, K. E. 2000 A novel mechanism for generating auxetic behaviour in reticulated foams: missing rib foam model. *Acta Mater.* **48**, 4349–4356. (doi:10.1016/S1359-6454(00)00269-X)
- Veronda, D. R., Westmann, R. A. 1970 Mechanical characterization of skin-finite deformations. *J. Biomech.* **3**, 111–24. (doi:10.1016/0021-9290(70)90055-2)
- Wadee, M. K., Wadee, M. A. & Bassom, A. P. 2007 Effects of orthotropy and variation of Poisson's ratio on the behaviour of tubes in pure flexure. *J. Mech. Phys. Solids* **55**, 1086–1102. (doi:10.1016/j.jmps.2006.10.003)
- Wojciechowski, K. W. 2003 Non chiral, molecular model of negative Poisson ratio in two dimensions. *J. Phys. A Math. Gen.* **36**, 11 765–11 778. (doi:10.1088/0305-4470/36/47/005)
- Wojciechowski, K. W. & Branka, A. C. 1989 Negative Poisson ratio in a two-dimensional 'isotropic' solid. *Phys. Rev. A* **40**, 7222–7225. (doi:10.1103/PhysRevA.40.7222)
- Wojciechowski, K. W. & Frenkel, D. 2004 Tetratic phase in the planar hard square system? *Comput. Meth. Sci. Technol.* **10**, 235–255.
- Yeganeh-Haeri, A., Weidner, D. J. & Parise, J. B. 1992 Elasticity of alpha-cristobalite—a silicon dioxide with a negative Poisson's ratio. *Science* **257**, 650–652. (doi:10.1126/science.257.5070.650)